American Journal of Pathology, Vol. 142, No. 6, June 1993

β/A4 Proteinlike Immunoreactive Granular Structures in the Brain of Senescence-Accelerated Mouse

Manabu Takemura,* Shinichi Nakamura,* Ichiro Akiguchi,* Masaki Ueno,* Nobuyuki Oka,* Shintaro Ishikawa,† Atsuyoshi Shimada,† Jun Kimura,* and Toshio Takeda†

From the Department of Neurology, Faculty of Medicine, and Department of Senescence Biology, Chest Disease Research Institute,† Kyoto University, Kyoto, Japan*

The immunohistochemical localization of amyloid β/A4 protein in the senescence-accelerated mouse brain was studied using six different antisera against human amyloid precursor protein peptides. β/A4 proteinlike immunoreactivity was observed in the form of granular structures (β-LIGS) in various regions, including the medial septum, cerebral cortex, hippocampus, cerebellum, and some cranial nerve roots. β-LIGS were 1.5 to 2.5 μ in diameter and irregularly shaped. They increased significantly in number with aging, predominantly in animals with a phenotype of age-related deterioration of memory and learning abilities. Congo red and thioflavine S did not stain the granules. On immunoblots, the main immunoreactive bands were observed at 14 to 18 kd. The staining intensities of these bands also increased with advancing age. We consider that β-LIGS are not only a new morphological manifestation of senescence in mice, but also a pertinent clue in understanding the mechanisms of amyloid deposition. (Am J Pathol 1993, 142: 1887–1897)

Amyloid β/A4 protein, a 4.2-kd polypeptide,[1,2] is the integral component of senile plaques and cerebrovascular amyloid fibrils in individuals with Alzheimer's disease,[3–5] Down's syndrome,[6] and normal aging.[7,8] Amyloid β/A4 protein seems to originate from amyloid precursor protein (APP), which has several species generated by alternative splicing.[9–14] Amyloid β/A4 protein deposition seen in subjects with Alzheimer's disease has been found only in higher mammalians such as primates, dogs, and polar bears.[15–22] Recently, two groups reported that transgenic mice and transplants of trisomy 16 mice could serve as experimental models for amyloid β/A4 protein deposition in the brain.[23,24]

The senescence-accelerated mouse (SAM), a murine model of accelerated senescence, has been established by Takeda and colleagues.[25,26] There are now eight accelerated senescence prone lines (SAM-P) and three accelerated senescence resistant lines (SAM-R), the latter with normal characteristics of aging. Each line has a relatively strain-specific pathological phenotype such as systemic senile amyloidosis,[27–30] senile cataract,[31] senile osteoporosis,[32] or degenerative joint disease.[33] SAM-P/8 shows early onset and rapid advancement of senescence revealed by analysis of aging dynamics such as Gompertz function, survivorship curve, and grading score system[34] and exhibits a significant age-related deterioration of memory and learning abilities.[35–38]

To our knowledge, there has been no report of a spontaneous development of β/A4 immunoreactivity in the mouse brain. In the present study, we examined immunohistochemically and immunochemically the SAM-P/8 brain and the SAM-R/1 brain, using six different antisera against synthetic or recombinant human APP peptides. We present here evidence indicating that β/A4-like immunoreactive structures occur in the SAM brain and show a marked age-related increase.

Materials and Methods

Animals

We examined five young (2-month-old), five middle-aged (9-month-old), and four old (12-month-old) SAM-P/8 and SAM-R/1 male mice, respectively, and

Accepted for publication January 11, 1993.

Address reprint requests to Dr. Toshio Takeda, Department of Senescence Biology, Chest Disease Research Institute, Kyoto University, 53 Shogoin Kawahara-cho, Sakyo-ku, Kyoto 606, Japan.

two very old (22-month-old) SAM-R/1 male mice. The mice were reared in our laboratory under conventional conditions at constant temperature (24 ± 2 C) and were maintained on a 7 A.M. to 7 P.M. light/7 P.M. to 7 A.M. dark schedule and on a commercial diet (CE-2, Nihon CLEA) and tap water *ad libitum*.

Tissues

The mice were deeply anesthesized with an intraperitoneal injection of 0.07 ml of 5% sodium pentobarbital and perfused transcardially with 50 ml ice-cold 0.01 mol/L phosphate-buffered saline (PBS, pH 7.4), followed by a fixative of 150 ml of 4% paraformaldehyde and 0.2% picric acid in 0.1 mol/L phosphate buffer (pH 7.4). The brains were removed immediately and soaked in a postfixative consisting of 4% paraformaldehyde and 0.2% picric acid in 0.1 mol/L phosphate buffer (pH 7.4). Following cryoprotection with 20% sucrose in 0.1 mol/L phosphate buffer (pH 7.4) overnight at 4 C, blocks were frozen and cut serially into 15-μ-thick sections on a freezing microtome.

Immunohistochemistry

The immunohistochemical staining was done using the avidin-biotin complex (Vector Laboratories, Burlingame, CA) method. Sections were kept in 0.3% H_2O_2 in 0.1 mol/L PBS for 30 minutes at room temperature to inhibit endogenous peroxidase activity. After rinsing with 0.1 mol/L PBS containing 0.3% Triton X-100 (PBST), they were incubated in a primary antibody diluted in PBST for 24 hours at 4 C. A rabbit polyclonal antibody raised against a synthetic human $\beta/A4_{1-24}$ peptide[39] (1:5,000), a rabbit polyclonal antibody against a human $\beta/A4_{1-42}$ peptide (Boehringer Mannheim Biochemica, Mannheim, Germany, 30 μg/ml), a rabbit polyclonal antibody against a synthetic human $\beta/A4_{1-15}$ (1:1,000), a rabbit polyclonal antibody against a recombinant human APP_{1-592}, which corresponds to 1–592 of APP_{695} (1:5,000), a rabbit polyclonal antibody against a synthetic human $APP_{671-695}$, which corresponds to C-terminal 25 amino acid residues of human APP_{695} (1:4,000), and a rabbit polyclonal antibody against a synthetic human $APP_{666-695}$[40] (1:1,000) were used as primary antibodies. After rinsing with PBST, sections were incubated in a biotinylated anti-rabbit IgG diluted (1:200) in PBST for 1 hour at room temperature. After washing with PBST, they were placed in an avidin-biotin peroxidase complex diluted (1:400) in PBST for 1 hour at room temperature. After washing thoroughly with 0.05 mol/L Tris-HCl buffer (pH 7.6), they were colored with 0.02% 3-3′ diaminobenzidine tetrahydrochloride, 0.45% nickel ammonium sulfate, and 0.006% H_2O_2 in 0.05 mol/L Tris-HCl (pH 7.6) for 10 minutes. These stained sections were then mounted onto gelatin-coated slides, air-dried, dehydrated within a graded series of ethanol, cleared by xylene, and coverslipped with Entellan new (Merck, Darmstadt, Germany). The immunohistochemical absorption experiment was done by adding 0.1 to 10 μmol/L $\beta/A4_{1-24}$ peptide to the working solution. As a control experiment, we performed the identical immunohistochemical procedure but with omission of the primary antibody or using a normal rabbit serum instead of the primary antibody. Some sections from all the animals were stained with hematoxylin and eosin, neutral red, Congo red, thioflavine S, and periodic acid-Schiff (PAS).

Immunoblotting Analysis

We examined SAM-P/8 and SAM-R/1 male mice of three age groups (2 months old, 9 months old, and 12 months old). We studied three mice for each age group. These mice were anesthesized and perfused transcardially with 50 ml ice-cold 0.01 mol/L PBS (pH 7.4). Each brain was homogenized at 4 C in 10 volumes of 0.01 mol/L PBS (pH 7.4). Homogenized samples were centrifuged at 30,000*g*, and pellets were resuspended in 3 to 5 volumes of 2% sodium dodecyl sulfate containing 8 mol/L urea. These resuspended samples were solubilized in 50-fold sodium dodecyl sulfate sample buffer as described by Laemmli,[41] incubated for 1 hour at 37 C, then sonicated. Diluted samples (15 to 20 μl) were electrophoresed on 8% or 20% polyacrylamide gels and transferred to polyviniliden difluoride filters (Immobilon, Nihon Millipore Co., Ltd., Tokyo, Japan). The transferred membranes were incubated in a blocking solution of 3% bovine serum albumin in 0.01 mol/L PBS (pH 7.2) and then in a primary antibody for 24 hours at 4 C. An anti-$\beta/A4_{1-24}$ antibody (1:3,000), an anti-$\beta/A4_{1-42}$ antibody (30 μg/ml), an anti-$\beta/A4_{1-15}$ antibody (1:1,000), and an anti-$APP_{671-695}$ antibody (1:2,000) were used as primary antibodies. After washing with 0.01 mol/L PBS (pH 7.4), the membranes were incubated in a biotinylated anti-rabbit IgG diluted (1:1,000) in 0.01 mol/L PBS (pH 7.4) for 1 hour at room temperature, washed again with 0.01 mol/L PBS (pH 7.4), and then reacted with an avidin-biotin peroxidase complex diluted (1:200) in 0.01 mol/L PBS (pH 7.4) for

30 minutes at room temperature. They were immersed in 0.005% 3-3′ diaminobenzidine tetrahydrochloride and 0.006% H_2O_2 in 0.05 mol/L Tris-HCl (pH 7.4).

Quantitative Analysis

Two sections of the cerebral cortex at the level of 2.6 to 2.8 mm rostral to the frontal zero plane, the vertical plane running through the interaural line, and two sections of the trigeminal nerve root at the level of 0.2 to 0.4 mm caudal to the frontal zero plane were collected from β/$A4_{1-24}$ immunostained sections of each animal. Four representative microscopic fields under a ×20 objective lens were arbitrarily selected bilaterally from each section. The immunoreactive granules in each field (3.72×10^4 μ^2) were counted using a computerized image analyzer, LUZEX3U (Nikon, Tokyo, Japan). The numerical densities (number/μ^2) were calculated. A statistical analysis was done using paired *t*-test to evaluate differences in the numerical densities of immunoreactive granules among respective age groups of both SAM-P/8 and SAM-R/1. Differences in the numerical densities of granules between age-matched SAM-P/8 and SAM-R/1 were also statistically analyzed by paired *t*-test.

Homology Search

To investigate the possibility of cross-reactivity of the present β/A4 antiserum with other homologous proteins, a homology search was performed using a computerized homology search system, Integrated Database and Extended Analysis System for Nucleic Acids and Proteins. Proteins with amino acid sequence homologous to the human β/$A4_{1-24}$ peptide were searched for among already known proteins of mammalians, including mouse, and the percent match was calculated.

Results

Histological Study

We found amyloid β/A4 proteinlike immunoreactivity in the form of a granular structure in various regions of the SAM brains, using an anti-β/$A4_{1-24}$ antibody (Figure 1). The β/A4-like immunoreactive granular structures (β-LIGS) were 1.5 to 2.5 μ in diameter and irregularly shaped. The topographic distribution of β-LIGS is shown in Figure 2. They were disseminated in both gray and white matter such as the lateral olfactory tract, medial septum, cerebral cortex, thalamus, hippocampus, caudate putamen, pyramidal tract, cerebellar peduncle, cerebellum, and some cranial nerve roots and nuclei. In the cerebral cortex, the granules were mainly observed in the deep cortical layers (Figure 1, A and B). In the hippocampus, two types of immunoreactive granules were observed (Figure 3A): β-LIGS and granules of a larger size. Larger granules were round to ovoid in shape. They were usually clustered and stained

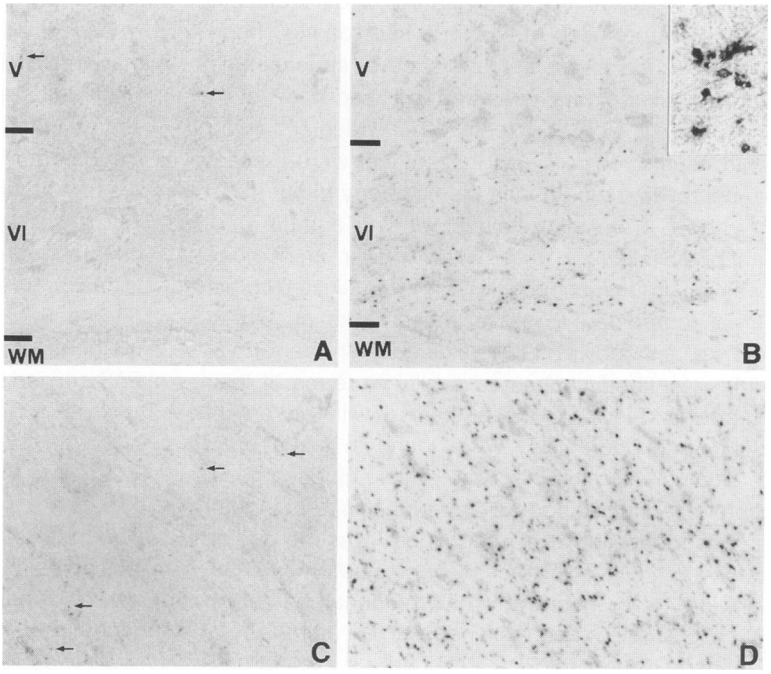

Figure 1. *Immunohistochemistry of the brains of SAM-P/8 using antiserum (1:5,000) against a synthetic human β/$A4_{1-24}$.* **A**: *Very few β-LIGS (arrows) are observed in the frontoparietal cortex of a 2-month-old SAM-P/8 mouse (×360).* **B**: *β-LIGS in the frontoparietal cortex of a 12-month-old SAM-P/8 mouse. Numerous granules are observed mainly in the deep cortical layers (×360). Inset shows a higher power view of β-LIGS (×1,000). V: fifth cortical layer, VI: sixth cortical layer, WM: white matter.* **C**: *β-LIGS (arrows) in the trigeminal nerve root of a 2-month-old SAM-P/8 mouse (×360).* **D**: *β-LIGS in the trigeminal nerve root of a 12-month-old SAM-P/8 mouse. Granules are markedly increased in number and are more strongly immunolabeled compared with those in a 2-month-old SAM-P/8 mouse (×360).*

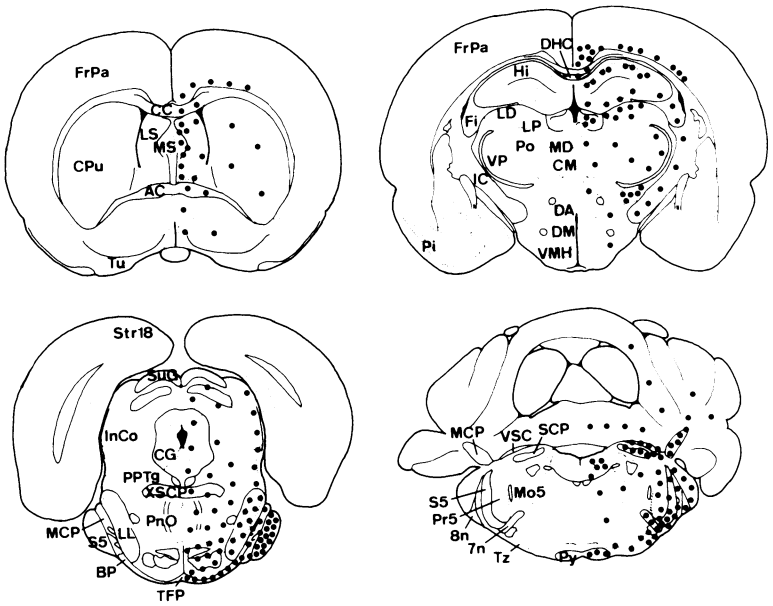

Figure 2. *Topographic distribution of β-LIGS in the brain of a 12-month-old SAM-P/8. β-LIGS are distributed in the various brain regions, including the medial septum, cerebral cortex, hippocampus, and some cranial nerve roots. FrPa: frontoparietal cortex, CPu: caudate putamen, CC: corpus callosum, MS: medial septal nucleus, LS: lateral septal nucleus, AC: anterior commissure, Tu: olfactory tubercle, DHC: dorsal hippocampal commissure, Hi: hippocampus, Fi: fimbria, MD: mediodorsal thalamic nucleus, CM: central medial thalamic nucleus, LD: laterodorsal thalamic nucleus, LP: lateral posterior thalamic nucleus, Po: posterior thalamic nucleus, VP: ventral posterior thalamic nucleus, DA: dorsal hypothalamic area, DM: dorsomedial hypothalamic nucleus, VMH: ventromedial hypothalamic nucleus, SuG: superficial gray layer of superior colliculus, INCo: intercollicular nucleus, CG: central gray, PPTg: pedunculopontine tegmental nucleus, XSCP: decussation of superior cerebellar peduncle, PnO: pontine reticular nucleus, TFP: transverse fibers of pons, LL: lateral lemniscus, BP: brachium pontis, MCP: middle cerebellar peduncle, S5: sensory root of trigeminal nerve, SCP: superior cerebellar peduncle, VSC: ventral spinocerebellar tract, Mo5: motor trigeminal nucleus, Pr5: principal sensory trigeminal nucleus, 7n: facial nerve, 8n: vestibulocochlear nerve, Tz: trapezoid body, Py: pyramidal tract.*

with PAS, findings compatible with previously reported PAS-positive granular structures (PGS).[42] PGS were also stained with various other antisera and even with normal rabbit serum (1:2,000). β-LIGS were stained only when we used frozen sections from perfused brains, in a free-floating condition. We found no immunoreactive structures in formalin-fixed paraffin-embedded sections, even with formic acid pretreatment.[43] Counterstaining with neutral red revealed that β-LIGS were present in neuropils rather than in the cell body (Figure 3B).

β-LIGS were also stained with an anti-β/$A4_{1-15}$ antibody, although they were smaller in number, weaker in immunopositivity and in limited brain areas compared to those stained with an anti-β/$A4_{1-24}$ antibody. β-LIGS stained with an anti-β/$A4_{1-15}$ antibody appeared similar in terms of their shape and size to those stained with an anti-β/$A4_{1-24}$ antibody. They were found in some brain areas including the cingulate cortex, hippocampus, cerebellar nuclei, cerebellar peduncles, and trigeminal and vestibular nuclei. There was no region where granular structures were stained only with an anti-β/$A4_{1-15}$ antibody. In the hippocampus, both β-LIGS and PGS were stained with an anti-β/$A4_{1-15}$ antibody. An anti-APP_{1-592} stained a subset of neurons, as described previously,[44,45] although β-LIGS were not stained (Figure 3C). An anti-$APP_{671-695}$, an anti-$APP_{666-695}$ and an anti-β/$A4_{1-42}$ antibodies did not label the β-LIGS despite formic acid pretreatment with various concentrations.[43,46]

Control staining was made by omission of the primary antibody or exchanging the primary antibody with normal rabbit serum. β-LIGS were never observed under these conditions. When sections were incubated in the primary antibody preabsorbed with 0.1 to 10 μmol/L synthetic human β/$A4_{1-24}$, no specific staining was observed (Figure 3D). The identical procedure also abolished senile plaque staining in the brain of a subject with Alzheimer's disease (Figure 3, E and F). Congo red or thioflavine S methods did not stain similar granular structures. PAS stained PGS but not β-LIGS.

Immunoblotting Analysis

For immunoblotting analysis, we used two gels with polyacrylamide concentrations of 8% and 20% to clearly separate the high molecular weight region, including full-length APP (120 to 130 kd), and the low molecular weight region, including β/A4 protein

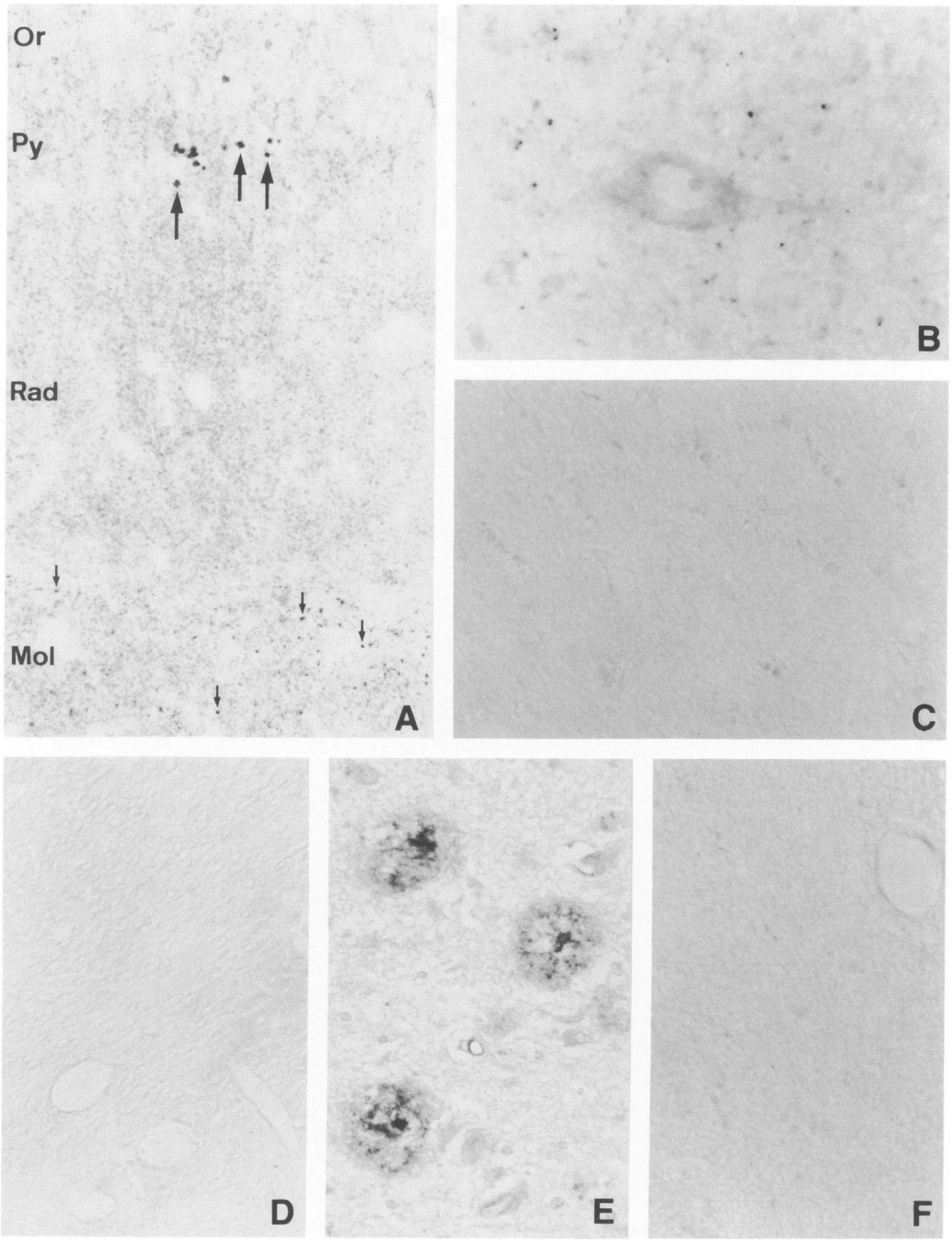

Figure 3. *Immunohistochemistry of the brain of a 12-month-old SAM-P/8 (*A *to* D*), and immunohistochemistry of the human brain of Alzheimer's disease as a positive control (*E *and* F*).* A: *In the hippocampus immunolabeled by anti-β/A4$_{1-24}$ antiserum (1:5,000), two types of immunoreactive granules are observed: the larger PGS (long arrows) and the smaller β-LIGS (short arrows) (×360). Or: oriens layer, Py: pyramidal cell layer, Rad: stratum radiatum, Mol: molecular layer.* B: *Counterstaining with neutral red suggests that granules are mainly localized in neuropils (×360).* C: *In the trigeminal nerve root immunolabeled by antiserum (1:5,000) against a recombinant APP$_{1-502}$, no granular structures are stained (×360).* D: *The trigeminal nerve root immunolabeled by anti-β/A4$_{1-24}$ antiserum after preabsorption with 1 μmol/L synthetic human β/A4$_{1-24}$. β-LIGS staining is abolished (×360).* E: *Human temporal cortex immunolabeled by anti-β/A4$_{1-24}$ antiserum (1:8,000, ×360).* F: *Human temporal cortex immunolabeled by anti-β/A4$_{1-24}$ antiserum after preabsorption with 1 μmol/L synthetic β/A4$_{1-24}$. Senile plaque staining is abolished (×360).*

(4.2 kd), respectively. With the 20% polyacrylamide gel, robust 14- to 18-kd immunoreactive bands were identified (Figure 4A). The predicted 4.2-kd band that corresponds to the human β/A4 protein was not detected. Using the 8% polyacrylamide gel, a robust band was observed at the end of the gel (Figure 4B). Thus, the molecular weight of the main immunoreactive protein was lower than that of the gel end, <30 kd, which was separated into 14- to 18-kd bands with the 20% gel (Figure 4A). A faint

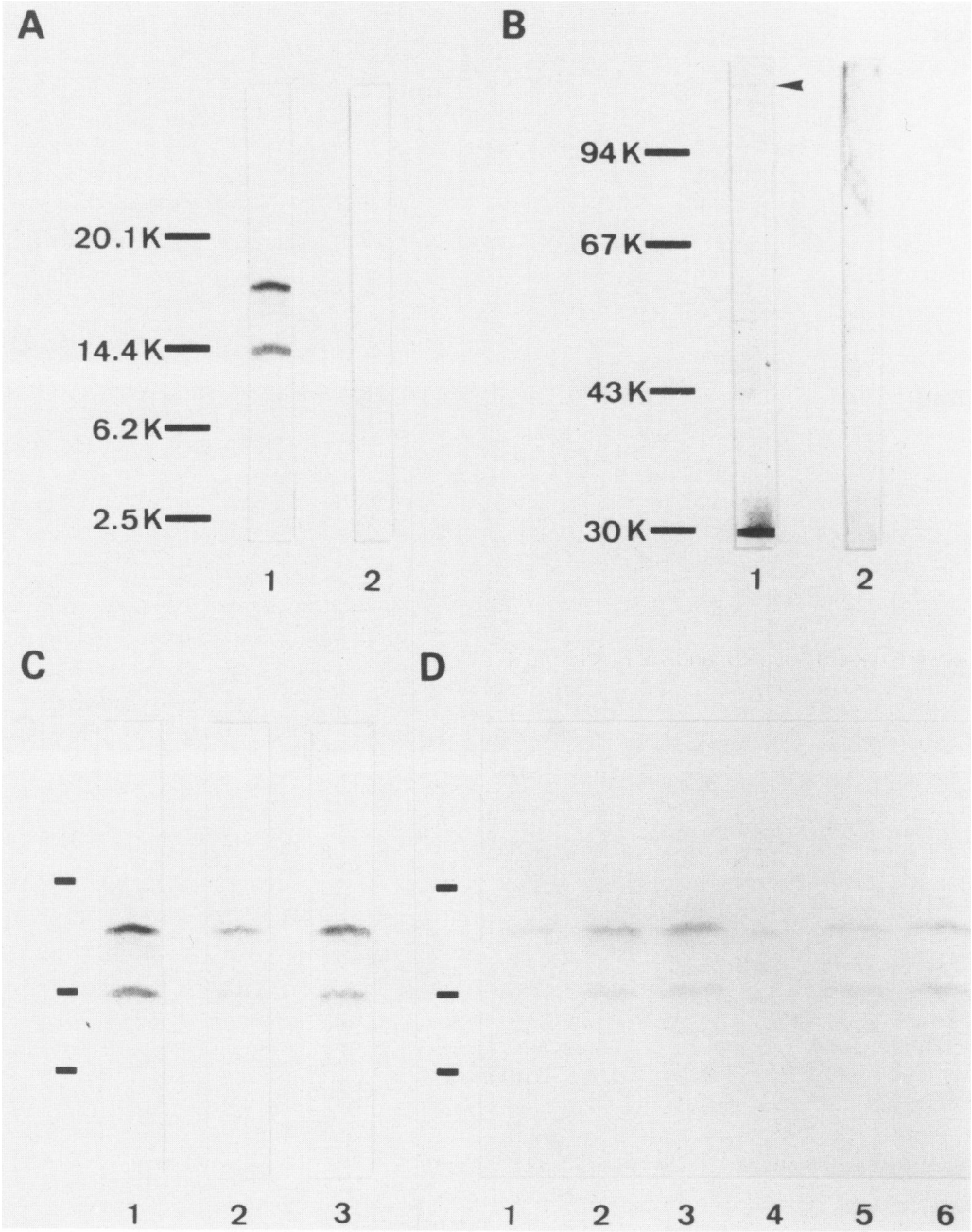

Figure 4. *Western immunoblots of the brains of SAM.* A: *Immunoblot of a 12-month-old SAM-P/8 using a 20% polyacrylamide gel.* Lane 1: *anti-β/A4$_{1-24}$ antiserum (1:3,000),* lane 2: *anti-β/A4$_{1-24}$ antiserum after absorption with 1 μmol/L synthetic β/A4$_{1-24}$. 14- to 18-kd bands are stained. The staining is abolished by preabsorption with the antigen.* B: *Immunoblot of a 12-month-old SAM-P/8 using a 8% polyacrylamide gel. A robust band at gel end (<30 kd) and a faint band at 120 kd (arrow head) are labeled. The labeling is abolished by preabsorption with the antigen.* Lane 1: *anti-β/A4$_{1-24}$ antiserum (1:3,000),* lane 2: *anti-β/A4$_{1-24}$ antiserum after absorption with 1 μmol/L synthetic β/A4$_{1-24}$.* C: *Immunoblots of a 12-month-old SAM-P/8 using a 20% polyacrylamide gels.* Lane 1: *anti-β/A4$_{1-24}$ antiserum (1:3,000),* lane 2: *anti-β/A4$_{1-42}$ antibody (30 μg/ml),* lane 3: *anti-APP$_{670-695}$ antiserum (1:2,000). All antibodies used here showed a similar immunoblotting pattern.* D: *Immunoblots of 2-, 9-, and 12-month-old SAM-P/8 and SAM-R/1 using an anti-β/A4$_{1-24}$ antiserum (1:3,000).* Lanes 1 *and* 4: *2-month-old,* lanes 2 *and* 5: *9-month-old,* lanes 3 *and* 6: *12-month-old SAM-P/8 (*lanes 1, 2, *and* 3*) and SAM-R/1 (*lanes 4, 5, *and* 6*). Staining intensities of immunoreactive bands seem to increase with aging in both SAM-P/8 and SAM-R/1. Increments of staining intensities occur in SAM-P/8 at a younger age than in SAM-R/1. 25 μg (*A *to* C*) or 15 μg (*D*) of total protein was applied to each lane. Bars indicate molecular weights: 20.1, 14.4, and 6.2 kd, respectively (*C *and* D*).*

120-kd band that seemed to be a full-length APP was also observed. Staining of these bands was abolished by preabsorption of the primary antibody with 1 to 10 μmol/L synthetic human β/A4$_{1-24}$ peptide (Figure 4, A, lane 2, and B, lane 2). The 14- to 18-kd bands were also recognized using an anti-β/A4$_{1-42}$ antibody, an anti-APP$_{671-695}$ antibody (Figure 4C), and an anti-β/A4$_{1-15}$ antibody as primary

antibodies. Staining intensities of immunoreactive bands increased with aging in both SAM-P/8 and SAM-R/1, and increases in staining intensities seemed to occur in the earlier life period in SAM-P/8 rather than in SAM-R/1 (Figure 4D).

Quantitative Analysis

β-LIGS seemed to be more numerous in the older animals in all regions where β-LIGS were observed, most prominent in the cerebral cortex, medial septum, thalamus, and trigeminal nerve root. We performed a quantitative analysis in the cerebral cortex and trigeminal nerve root using a computerized image analyzer, LUZEX3U (Figure 5). The mean numerical densities of β-LIGS in 2-, 4-, 9-, 12-, and 22-month-old SAM-R/1 were 0.13, 4.93, 33.5, 40.1, and 53.6 ($\times 10^{-4}/\mu^2$) in the cerebral cortex and 33.7, 46.5, 91.7, 97.3, and 107.6 ($\times 10^{-4}/\mu^2$) in the trigeminal nerve root, respectively. The mean numerical densities of β-LIGS in 2-, 4-, 9-, and 12-month-old SAM-P/8 were 0.24, 5.38, 59.0, and 75.1 ($\times 10^{-4}/\mu^2$) in the cerebral cortex and 34.9, 51.0, 111.0, and 126.3 ($\times 10^{-4}/\mu^2$) in the trigeminal nerve root, respectively. Differences in numerical densities between 2-month-old SAM-R/1 versus 9-, 12-, and 22-month-old SAM-R/1 were statistically significant at *P* values of 0.0532 (t = −4.159), 0.0082 (t = −10.974), and 0.0591 (t = −10.744) in the cerebral cortex and at *P* values of 0.0005 (t = −10.465), 0.0001 (t = −18.621), and 0.0235 (t = −27.109) in the trigeminal nerve root. Differences in numerical densities between 2-month-old SAM-P/8 versus 4-, 9-, and 12-month-old SAM-P/8 were also statistically significant at *P* values of 0.0163 (t = −7.732), 0.0001 (t = −25.34), and 0.0027 (t = −9.236) in the cerebral cortex and at *P* values of 0.0143 (t = −4.144), 0.0006 (t = −7.713), and 0.0009 (t = −8.776) in the trigeminal nerve root, respectively. In addition, in the cerebral cortex, differences in numerical densities of β-LIGS were statistically significant at a *P* value of 0.0386 (t = 3.533) for 9-month-old SAM-P/8 versus SAM-R/1 and at a *P* value of 0.0029 (t = 6.478) for 12-month-old SAM-P/8 versus 12-month-old SAM-R/1. In the trigeminal nerve root, the difference was statistically significant at a *P* value of 0.0354 (t = 3.124) for 12-month-old SAM-P/8 versus 12-month-old SAM-R/1.

Homology Search

The Integrated Database and Extended Analysis System for Nucleic Acids and Proteins revealed that

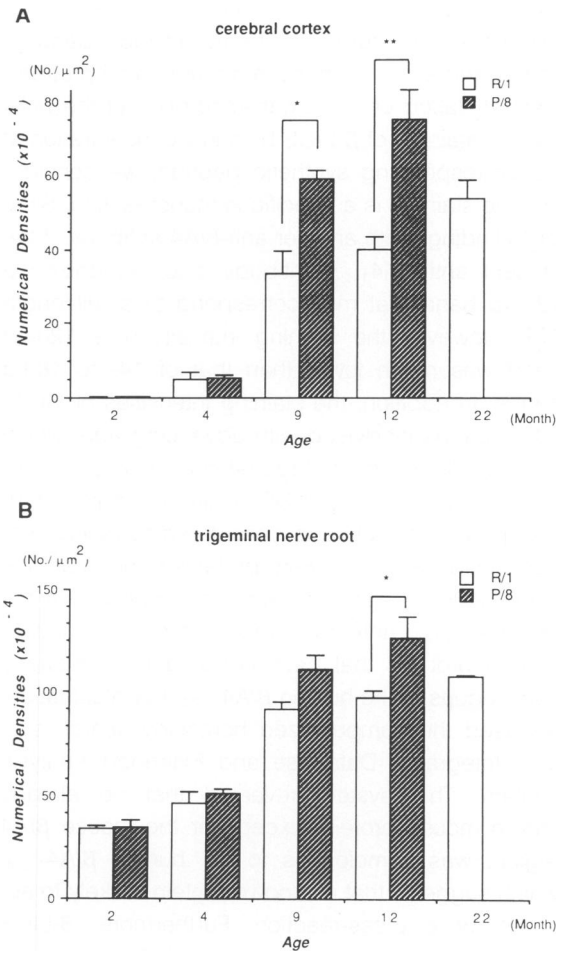

Figure 5. *Numerical densities of β-LIGS in the cerebral cortex (A) and the trigeminal nerve root (B). Numerical densities of β-LIGS increase significantly with advancing age in both SAM-R/1 and SAM-P/8 mice brains. Compared with 2-month-old SAM-R/1, increases in numerical densities of β-LIGS in 9-, 12-, and 22-month-old SAM-R/1 are statistically significant at* P *values of 0.0532, 0.0082, and 0.0591 in the cerebral cortex, and at* P *values of 0.0005, 0.0001, and 0.0235 in the trigeminal nerve root, respectively. Similarly, compared with 2-month-old SAM-P/8, increases in 4-, 9-, and 12-month-old SAM-P/8 are significant at* P *values of 0.0163, 0.0001, and 0.0027 in the cerebral cortex, and at* P *values of 0.0143, 0.0006, and 0.0009 in the trigeminal nerve root. In addition, increases in numerical densities of β-LIGS are more marked in SAM-P/8 compared with SAM-R/1 (*: P < 0.05, **: P < 0.01*). Each statistical analysis was done using paired* t*-test. Each bar represents mean ± SE.*

the mouse β/A4 region was 83.3% homologous to the human $\beta/A4_{1-24}$. No established mouse protein, except for the mouse β/A4 region, was found to be homologous to the human $\beta/A4_{1-24}$.

Discussion

To our knowledge, this is the first report of spontaneous development of β/A4-like immunoreactivity in the mouse brain. β-LIGS were stained only when we used frozen sections from perfused brains, in a

free-floating condition. We found no β/A4-like immunoreactive structures in formalin-fixed, paraffin-embedded sections, despite a formic acid pretreatment.[43] Based on the clear absorption of the β/A4 immunostaining of β-LIGS by a low concentration of the corresponding synthetic peptide, we consider that the staining is a specific immunoreaction. Similar to findings with another anti-β/A4 antibody,[44] the present anti-$\beta/A4_{1-24}$ antibody also recognized a 120-kd band that may correspond to a full-length APP. However, the staining intensity of a 120-kd band was much lower than that of 14- to 18-kd bands. In addition, the staining intensities of 14- to 18-kd bands increased with advancing age, which is compatible with the age-related increase in numerical densities of β-LIGS. Thus, the main immunoreactivity of β-LIGS is considered to reflect recognition of the 14- to 18-kd proteins rather than full-length APP. It is also possible to suppose that the anti-$\beta/A4_{1-24}$ antibody recognizes APP-unconcerned proteins that have amino acid sequences homologous to the human $\beta/A4_{1-24}$. For elucidation, we used the computerized homology search system, Integrated Database and Extended Analysis System. This system revealed that no already known mouse protein, except for the mouse β/A4 region, was homologous to the human $\beta/A4_{1-24}$, which suggests that no known protein is likely to account for a cross-reaction. Furthermore, β-LIGS were stained not only with an anti-$\beta/A4_{1-24}$ antibody but also with an anti-$\beta/A4_{1-15}$ antibody, and both antibodies recognized the same 14- to 18-kd bands on immunoblotting lanes. Thus, we consider that the possibility of a cross-reaction is unlikely, whereas we could not still exclude some possibility of an immunochemical or immunohistochemical cross-reaction with unknown protein.

An anti-$\beta/A4_{1-42}$ antibody and an anti-$APP_{671-695}$ antibody did not stain β-LIGS immunohistochemically, whereas they recognized the 14- to 18-kd bands on immunoblotting lanes. This discrepancy might be attributed to differences of epitopes recognized by each antibody. In tissue sections, epitopes recognized by an anti-$\beta/A4_{1-42}$ antibody or an anti-$APP_{671-695}$ antibody might be hidden due to conformations of the target protein or surrounding structures, whereas epitopes recognized by an anti-$\beta/A4_{1-24}$ antibody or an anti-$\beta/A4_{1-15}$ antibody were exposed using the present immunohistochemical procedure. In contrast, when we homogenized samples, these architectures might be broken down and epitopes exposed to be recognized by each antibody.

There has been no report on granular structure in the mouse brain similar to β-LIGS. PGS, described by Akiyama et al,[42] are granules of a larger size, measuring up to 5 μ, are usually clustered, and stain with PAS. In addition, immunohistochemically, PGS stained not only with the present anti-$\beta/A4_{1-24}$ antibody, but also with various others, including anti-APP_{1-592} antibody (1:3,000) and even with normal rabbit serum (1:2,000). Thus, we conclude that β-LIGS and PGS are dissimilar.

Numerical densities of β-LIGS increased significantly with advancing age in brains of both SAM-P/8 and SAM-R/1, characteristics of importance because only neuroaxonal dystrophies and eosinophilic thalamic intraneuronal inclusions,[47] lipofuscin accumulation,[48] and PGS[42] have been found as morphological parameters of aging in the mouse brain. Furthermore, numerical densities of β-LIGS increased more markedly in brains of SAM-P/8 compared with those of SAM-R/1. Increases in numerical densities of β-LIGS were most rapid at ages from 4 to 9 months. Studies on memory and learning abilities using both active and passive avoidance tasks showed that the deterioration of abilities progressed from age 4 to age 8/9 months[35–38] in SAM-P/8. Thus, the rapid and accelerated accumulation of β-LIGS might be associated with the age-related deterioration of memory and learning abilities seen in SAM-P/8.

As described above, the immunoreactivity of β-LIGS may be associated with the 14- to 18-kd proteins. Because the 14- to 18-kd proteins were specifically recognized with anti-β/A4 antibody, the 14- to 18-kd proteins seem to be the β/A4 region-containing APP fragments generated by normal or aberrant processing associated with aging. Moreover, certain parts of these fragments may harbor the C-terminal region of APP, according to the result of immunoblot using an anti-$APP_{671-695}$ antibody. As the identical anti-$\beta/A4_{1-24}$ antibody used in the present study recognized a 4.2-kd robust band in the brain of a subject with Alzheimer's disease,[39] processing of APP may occur in a different manner between mouse and human brains. Differences in the primary structure of APP[21,49,50] or the processing enzyme may relate to the differences in the processed proteins, 4.2-kd β/A4 protein in the human brain and 14- to 18-kd APP fragments in the mouse brain. The differences in the processed proteins could affect their polymerization into the β-pleated sheet,[51] leading to the development of characteristic senile plaques classically with Congo red birefringence in the human brain and to the development of granular deposits in the absence of Congo

red birefringence in the mouse brain. The characterization of the 14- to 18-kd proteins in the mouse brain is necessary to address this assumption.

In the present study, we obtained evidence indicating that β-LIGS, which may have 14- to 18-kd APP fragments as a component, develop spontaneously in the SAM brain and that they increase in number with advancing age, predominantly in animals with a phenotype of age-related deterioration of memory and learning abilities. We suggest that β-LIGS are not only a new morphological manifestation of senescence in mice brains, but also a pertinent clue to determine mechanisms involved in amyloid deposition.

Acknowledgments

We thank Drs. N. Kitaguchi and Y. Tokushima (Bioscience Laboratory, Life Science Research Laboratories, Asahi Chemical Industry Co., Ltd., Japan) for generous gifts of anti-β/$A4_{1-24}$ and anti-APP_{1-592} antibodies. We are grateful to Dr. K. Yoshikawa (Tokyo Metropolitan Institute for Neuroscience, Japan) for provision of anti-$APP_{671-695}$ antibody and to Dr. H. Yamaguchi (Gunma University school of medicine) for anti-β/$A4_{1-15}$ and anti-$APP_{666-695}$ antibodies with pertinent advice. We thank Drs. J. Tateishi, T. Kitamoto (Kyushu University), K. Higuchi, and Y. Ashida (Kyoto University) for pertinent advice and Miss Y. Kitasaka for technical assistance.

References

1. Bobin SA, Currie JR, Merz PA, Miller DL, Styles J, Walker WA, Wen GY, Wisniewski HM: The comparative immunoreactivities of brain amyloids in Alzheimer's disease and scrapie. Acta Neuropathol 1987, 74:313–323
2. Castano EM, Ghiso J, Prelli F, Gorevic PD, Migheli A, Frangione B: In vitro formation of amyloid fibrils from two synthetic peptides of different lengths homologous to Alzheimer's disease β-protein. Biochem Biophys Res Commun 1986, 141:782–789
3. Glenner GG, Wong CW: Alzheimer's disease: initial report of the purification and characterization of a novel cerebrovascular amyloid protein. Biochem Biophys Res Commun 1984, 120:885–890
4. Masters CL, Simms G, Weinman NA, Multhaup G, McDonald BL, Beyreuther K: Amyloid plaque core protein in Alzheimer disease and Down syndrome. Proc Natl Acad Sci USA 1985, 82:4245–4249
5. Selkoe DJ, Abraham CR, Podlisny MB, Duffy LK: Isolation of low-molecular-weight proteins from amyloid plaque fibers in Alzheimer's disease. J Neurochem 1986, 46:1820–1834
6. Glenner GG, Wong CW: Alzheimer's disease and Down's syndrome: sharing of a unique cerebrovascular amyloid fibril protein. Biochem Biophys Res Commun 1984, 122:1131–1135
7. Coria F, Castano EM, Frangione B: Brain amyloid in normal aging and cerebral amyloid angiopathy is antigenically related to Alzheimer's disease β-protein. Am J Pathol 1987, 129:422–428
8. Joachim CL, Duffy LK, Morris JH, Selkoe DJ: Protein chemical and immunocytochemical studies of meningovascular β-amyloid protein in Alzheimer's disease and normal aging. Brain Res 1988, 474:100–111
9. Kang J, Lemaire HG, Unterbeck A, Salbaum JM, Masters CL, Grzeschik KH, Multhaup G, Beyreuther K, Mueller-Hill B: The precursor of Alzheimer's disease amyloid A4 protein resembles a cell-surface receptor. Nature 1987, 325:733–736
10. Ponte P, Gonzalez-DeWhitt P, Schilling J, Miller J, Hsu D, Greenberg B, Davis K, Wallace W, Lieberburg I, Fuller F, Cordell B: A new A4 amyloid mRNA contains a domain homologous to serine proteinase inhibitors. Nature 1988, 331:525–527
11. Tanzi RE, McClatchey AI, Lamperti ED, Villa-Komaroff L, Gusella JF, Neve RL: Protease inhibitor domain encoded by an amyloid protein precursor mRNA associated with Alzheimer's disease. Nature 1988, 331:528–530
12. Kitaguchi N, Takahashi Y, Tokushima Y, Shiojiri S, Ito H: Novel precursor of Alzheimer's disease amyloid protein shows protease inhibitory activity. Nature 1988, 331:530–532
13. De Sauvage F, Octave JN: A novel mRNA of the A4 amyloid precursor gene coding for a possibly secreted protein. Science 1989, 245:651–653
14. Golde TE, Estus S, Usiak M, Younkin LH, Younkin SG: Expression of β amyloid protein precursor mRNAs: recognition of a novel alternatively spliced form and quantitation in Alzheimer's disease using PCR. Neuron 1990, 4:253–267
15. Wisniewski HM, Johnson AB, Raine CS, Kay WJ, Terry RD: Senile plaques and cerebral amyloidosis in aged dogs: a histochemical and ultrastructural study. Lab Invest 1970, 23:287–296
16. Wisniewski HM, Ghetti B, Terry RD: Neuritic (senile) plaques and filamentous changes in aged rhesus monkeys. J Neuropathol Exp Neurol 1973, 32:566–584
17. Struble RG, Price DL Jr, Cork LC, Price DL: Senile plaques in cortex of aged normal monkeys. Brain Res 1985, 361:267–275
18. Selkoe DJ, Bell DS, Podlisny MB, Price DL, Cork LC: Conservation of brain amyloid proteins in aged mammals and humans with Alzheimer's disease. Science 1987, 235:873–877
19. Abraham CR, Selkoe DJ, Potter H, Price DL, Cork LC: α_1-Antichymotrypsin is present together with the β-protein in monkey brain amyloid deposits. Neuroscience 1989, 32:715–720

20. Giaccone G, Verga L, Finazzi M, Pollo B, Tagliavini F, Frangione B, Bugiani O: Cerebral preamyloid deposits and congophilic angiopathy in aged dogs. Neurosci Lett 1990, 114:178–183
21. Podlisny MB, Tolan DR, Selkoe DJ: Homology of the amyloid beta protein precursor in monkey and human supports a primate model for beta amyloidosis in Alzheimer's disease. Am J Pathol 1991, 138:1423–1435
22. Ishihara T, Gondo T, Takahashi M, Uchino F, Ikeda S, Allsop D, Imai K: Immunohistochemical and immunoelectron microscopical characterization of cerebrovascular and senile plaque amyloid in aged dogs' brains. Brain Res 1991, 548:196–205
23. Quon D, Wang Y, Catalano R, Scardina JM, Murakami K, Cordell B: Formation of β-amyloid protein deposits in brains of transgenic mice. Nature 1991, 352:239–241
24. Richards SJ, Waters JJ, Beyreuther K, Masters CL, Wischik CM, Sparkman DR, White CL III, Abraham CR, Dunnett SB: Transplants of mouse trisomy 16 hippocampus provide a model of Alzheimer's disease neuropathology. EMBO J 1991, 10:297–303
25. Takeda T, Hosokawa M, Takeshita S, Irino M, Higuchi K, Matsushita T, Tomita Y, Yasuhira K, Hamamoto H, Shimizu K, Ishii M, Yamamuro T: A new murine model of accelerated senescence. Mech Ageing Dev 1981, 17:183–194
26. Takeda T, Hosokawa M, Higuchi K: Senescence-Accelerated Mouse (SAM): a novel murine model of accelerated senescence. J Am Geriatr Soc 1991, 39: 911–919
27. Matsumura A, Higuchi K, Shimizu K, Hosokawa M, Hashimoto K, Yasuhira K, Takeda T: A novel amyloid fibril protein isolated from Senescence-Accelerated Mice. Lab Invest 1982, 47:270–275
28. Higuchi K, Yonezu T, Kogishi K, Matsumura A, Takeshita S, Higuchi K, Kohno A, Matsushita M, Hosokawa M, Takeda T: Purification and characterization of a senile amyloid-related antigenic substance ($apoSAS_{SAM}$) from mouse serum. J Biol Chem 1986, 261:12834–12840
29. Yonezu T, Tsunasawa S, Higuchi K, Kogishi K, Naiki H, Hanada K, Sakiyama F, Takeda T: A molecular-pathologic approach to murine senile amyloidosis: serum precursor-apolipoprotein A-II valiant ($Pro^5 \rightarrow Gln$) presents only in the senile amyloidosis-prone SAM-P/1 and SAM-P/2 mice. Lab Invest 1987, 57:65–70
30. Naiki H, Higuchi K, Yonezu T, Hosokawa M, Takeda T: Metabolism of senile amyloid procursor and amyloidogenesis: age-related acceleration of apolipoprotein A-II clearance in the Senescence Accelerated Mouse. Am J Pathol 1988, 130:579–587
31. Hosokawa M, Takeshita S, Higuchi K, Shimizu K, Irino M, Toda K, Honma A, Matsumura A, Yasuhira K, Takeda T: Cataract and other ophthalmic lesions in Senescence Accelerated Mouse (SAM). Morphology and incidence of senescence associated ophthalmic changes in mice. Exp Eye Res 1984, 38:105–114
32. Matsushita M, Tsuboyama T, Kasai R, Okumura H, Yamamuro T, Higuchi K, Higuchi K, Kohno A, Yonezu T, Utani A, Umezawa M, Takeda T: Age-related changes in bone mass in the Senescence-Accelerated Mouse (SAM): SAM-R/3 and SAM P/6 as new murine models for senile osteoporosis. Am J Pathol 1986, 125:276–283
33. Chen WH, Hosokawa M, Tsuboyama T, Ono T, Iizuka T, Takeda T: Age-related changes in the temporomandibular joint of the Senescence Accelerated Mouse. Am J Pathol 1989, 135:379–385
34. Hosokawa M, Kasai R, Higuchi K, Takeshita S, Shimizu K, Hamamoto H, Honma A, Irino M, Toda K, Matsumura A, Matsushita M, Takeda T: Grading score system: a method for evaluation of the degree of senescence in Senescence Accelerated Mouse (SAM). Mech Ageing Dev 1984, 26:91–102
35. Miyamoto M, Kiyota Y, Yamazaki N, Nagaoka A, Matsuo T, Nagawa Y, Takeda T: Age-related changes in learning and memory in the Senescence-Accelerated Mouse (SAM). Physiol Behav 1986, 38:399–406
36. Yagi H, Katoh S, Akiguchi I, Takeda T: Age-related deterioration of ability of acquisition in memory and learning in senescence accelerated mouse: SAM-P/8 as an animal model of disturbances in recent memory. Brain Res 1988, 474:86–93
37. Yagi H, Irino M, Matsushita T, Katoh S, Umezawa M, Tsuboyama T, Hosokawa M, Akiguchi I, Tokunaga R, Takeda T: Spontaneous spongy degeneration of the brain stem in SAM-P/8 mice, a newly developed memory-deficient strain. J Neuropathol Exp Neurol 1989, 48:577–590
38. Ohta A, Hirano T, Yagi H, Tanaka S, Hosokawa M, Takeda T: Behavioral characteristics of the SAM-P/8 strain in Sidman active avoidance task. Brain Res 1989, 498:195–198
39. Takahashi H, Kurashima C, Utsuyama M, Hirokawa K: Immunohistological study of senile brains by using a monoclonal antibody recognizing β amyloid precursor protein: significance of granular deposits in relation with senile plaques. Acta Neuropathol 1990, 80:260–265
40. Yamaguchi H, Ishiguro K, Shoji M, Yamazaki T, Nakazato Y, Ihara Y, Hirai S: Amyloid β/A4 protein precursor is bound to neurofibrillary tangles in Alzheimer-type dementia. Brain Res 1990, 537:318–322
41. Laemmli UK: Cleavage of structural proteins during the assembly of the head of bacteriophage T4. Nature 1970, 227:680–685
42. Akiyama H, Kameyama M, Akiguchi I, Sugiyama H, Kawamata T, Fukuyama H, Kimura H, Matsushita M, Takeda T: Periodic acid-Schiff (PAS)-positive, granular structures increase in the brain of senescence accelerated mouse (SAM). Acta Neuropathol 1986, 72:124–129

43. Kitamoto T, Ogomori K, Tateishi J, Prusiner SB: Formic acid pretreatment enhances immunostaining of cerebral and systemic amyloids. Lab Invest 1987, 57:230–236
44. Card JP, Meade RP, Davis LG: Immunocytochemical localization of the precursor protein for β-amyloid in the rat central nervous system. Neuron 1988, 1:835–846
45. Kawarabayashi T, Shoji M, Harigaya Y, Yamaguchi H, Hirai S: Amyloid β/A4 protein precursor is widely distributed in both the central and peripheral nervous systems of the mouse. Brain Res 1991, 552:1–7
46. Perry G, Cras P, Siedlak SL, Tabaton M, Kawai M: β protein immunoreactivity is found in the majority of neurofibrillary tangles of Alzheimer's disease. Am J Pathol 1992, 140:283–290
47. Fraser H: Eosinophilic bodies in some neurones in the thalamus of ageing mice. J Pathol 1969, 98:201–204
48. Nandy K, Bourne GH: Effect of centrophenoxine on the lipofuscin pigments in the neurones of senile guinea-pigs. Nature 1966, 210:313–314
49. Yamada T, Sasaki H, Furuya H, Miyata T, Goto I, Sakaki Y: Complementary DNA for the mouse homolog of the human amyloid beta protein precursor. Biochem Biophys Res Commun 1987, 149:665–671
50. Yamada T, Sasaki H, Doh-ura K, Goto I, Sakaki Y: Structure and expression of the alternatively-spliced forms of mRNA for the mouse homolog of Alzheimer's disease amyloid beta protein precursor. Biochem Biophys Res Commun 1989, 158:906–912
51. Kirschner DA, Inouye H, Duffy LK, Sinclair A, Lind M, Selkoe DJ: Synthetic peptide homologous to β protein from Alzheimer disease forms amyloid-like fibrils in vitro. Proc Natl Acad Sci USA 1987, 84:6953–6957